Chen, E. Y., & Seeburg, P. H. (1985) *DNA 4*, 165–170.
Dahl, H. H. M., & Mercer, J. F. B. (1986) *J. Biol. Chem. 261*, 4148–4153.
DiLella, A. G., Kwok, S. C. M., Ledley, F. D., Marvit, J., & Woo, S. L. C. (1986) *Biochemistry 25*, 743–749.
Egeland, J. A., Gerhard, D. S., Pauls, D. L., Sussex, J. N., Kidd, K. K., Allen, C. R., Hostetter, A. M., & Housman, D. E. (1987) *Nature (London) 325*, 783–787.
Ginns, E. D., Kelsoe, J. R., Martin, B. M., Winfield, S. L., LaMarca, M. E., Luu, M. D., Paul, S. M., & O'Malley, K. L. (1987) *Soc. Neurosci. Abstr. 13*, 856.
Goodman, R., & Herschman, H. R. (1978) *Proc. Natl. Acad. Sci. U.S.A. 75*, 4587–4590.
Grima, B., Lamouroux, A., Blanot, F., Faucon-Biquet, N., & Mallet, J. (1985) *Proc. Natl. Acad. Sci. U.S.A. 73*, 617–621.
Grima, B., Lamouroux, A., Boni, C., Julien, J.-F., Javoy-Agid, F., & Mallet, J. (1987) *Nature (London) 326*, 707–711.
Harrington, C. A., Lewis, E. J., Krzemien, D., & Chikaraishi, D. M. (1987) *Nucleic Acids Res. 15*, 2363–2387.
Kaneda, N., Kobayashi, K., Ichinose, H., Kishi, F., Nakazawa, A., Kurosawa, Y., Fujita, K., & Nagatsu, T. (1987) *Biochem. Biophys. Res. Commun. 146*, 971–975.
Ledley, F. D., DiLella, A. G., Kwok, S. C. M., & Woo, S. L. C. (1985) *Biochemistry 24*, 3394–3397.
Leff, S. L., Rosenfeld, M. G., & Evans, R. M. (1986) *Annu. Rev. Biochem. 55*, 1091–1117.
Lewis, E. J., Harrington, C. A., & Chikaraishi, D. M. (1987) *Proc. Natl. Acad. Sci. U.S.A. 84*, 3550–3554.
Maniatis, T., Fritsch, E. F., & Sambrook, M. (1982) *Molecular Cloning: A Laboratory Manual*, Cold Spring Harbor Laboratory, Cold Spring Harbor, NY.
McTigue, M., Cremins, J., & Halegoua, S. (1985) *J. Biol. Chem. 260*, 9047–9056.
Moss, P. A. H., Davies, K. R., Boni, C., Mallet, J., & Reeders, S. T. (1986) *Nucleic Acids Res. 14*, 9927–9932.
Mount, S. M. (1982) *Nucleic Acids Res. 10*, 459–472.
Ohshima, Y., & Gotoh, Y. (1987) *J. Mol. Biol. 195*, 247–259.
O'Malley, K. L. (1986) *J. Neurosci. Res. 16*, 3–12.
Smith, G. E., Ju, G., Ericson, B. L., Moschera, J., Lahm, H.-W., Chizzonite, R., & Summers, M. D. (1985) *Proc. Natl. Acad. Sci. U.S.A. 82*, 8404–8408.
Smith, H. O., & Birnstiel, M. L. (1975) *Nucleic Acids Res. 3*, 2387–2395.
Thoenen, H. (1974) *Life Sci. 14*, 223–235.
Vadasz, C., Baker, H., Fink, S. J., & Reis, D. J. (1985) *J. Neurogenet. 2*, 219–230.
Wagner, C. E., & O'Malley, K. L. (1987) *Proc. Int. Catecholamine Symp., 6th* (in press).
Wahl, G. M., Stern, M., & Stark, G. R. (1979) *Proc. Natl. Acad. Sci. U.S.A. 76*, 3683–3687.
Zigmond, R. E., Schon, F., & Iversen, L. L. (1974) *Brain Res. 70*, 547–552.

Chemical Relaxation in a Chemiosmotic-Coupled System: Driving the Calcium Adenosinetriphosphatase with Bacteriorhodopsin†

X. L. Wu and T. G. Dewey*
Department of Chemistry, University of Denver, Denver, Colorado 80208
Received August 5, 1987; Revised Manuscript Received September 4, 1987

ABSTRACT: Phase-lifetime spectroscopy has been used to measure chemical relaxation processes in a chemiosmotic-coupled system. In this experiment the calcium ATPase and bacteriorhodopsin were coreconstituted into phospholipid vesicles. Upon illumination the bacteriorhodopsin pumps protons into the vesicles and forms a membrane potential. This membrane potential alters the activity of the internal calcium and thus perturbs the equilibrium of ATP hydrolysis/synthesis coupled to calcium transport. Mechanically chopping the actinic light provides a periodic perturbation to the system, and small response signals can be observed by using phase-sensitive detection. It is shown that this periodic perturbation occurs about a steady-state membrane potential that is independent of chopping frequency. The amplitude dispersion curve for the fluorescence of a calcium indicator was observed and analyzed in terms of the relaxation time for the ATPase-catalyzed calcium transport. Thus, this technique provides a method of measuring ion transport kinetics against a constant chemiosmotic potential. The calcium ATPase showed a single relaxation time on this time scale. The dependence of this relaxation time on ADP and phosphate concentration was measured and analyzed with a random sequential mechanism. This analysis gave dissociation constants for ADP and phosphate of 3.2 mM and 1.4 mM, respectively. These binding steps are followed by slow isomerization steps with forward and reverse rate constants (in the direction of ATP synthesis) of 67 s^{-1} and 227 s^{-1}, respectively. These results demonstrate that highly accurate kinetic data can be obtained with this modulation relaxation technique.

Knowledge of the rates of the individual, elementary reaction steps is required for a detailed, molecular description of ion transport across biological membranes. Such information has proven to be unusually difficult to obtain for even the best characterized membrane-bound transport proteins. This is, in part, due to a lack of high-resolution kinetic techniques for measuring ion transport against a constant chemiosmotic potential. Large changes in the chemiosmotic

† This work was supported by a grant from the National Science Foundation (DMB-8703860).
* Author to whom correspondence should be addressed.

0006-2960/87/0426-6914$01.50/0

potential occur in most stopped-flow and stopped-quench experiments because the internal volumes of the vesicles are too small to effectively buffer the concentration of the transported species. Thus, the energetics of transport is changing dramatically during the time course of the experiments. A limited number of flash experiments aimed at measuring coupled proton transport processes have been performed on chloroplast thylakoids (Auslaender & Junge, 1975). This is a complex system with numerous technical difficulties. A problem with many flash experiments is that high-intensity actinic flashes are required, and this may not represent a small perturbation on the system. Other conventional relaxation techniques such as temperature jump have not been attempted. The difficulty with such methods is that the system must be poised about equilibrium or steady-state conditions. This is extremely difficult to achieve in most chemiosmotic-coupled ATPase[1] systems because of uncoupled ATP hydrolysis activity [cf. Hasselbach (1978)]. Therefore, any relaxation experiment would require that the gradient be maintained by an external source. Tsong and co-workers have used electric field jump techniques to measure ATP synthesis in chemiosmotic systems (Tsong & Astumian, 1986; Knox & Tsong, 1984). While this is a promising approach, to date it has not provided detailed kinetic information.

In this work modulation relaxation spectroscopy (Dewey & Hammes, 1981a; Hasselbacher et al., 1986) is further developed to investigate ion transport catalyzed by the calcium ATPase. This method is a periodic perturbation technique, which allows the measurement of ion fluxes against a constant, steady-state chemiosmotic potential. In these experiments the calcium ATPase is reconstituted into phospholipid vesicles along with bacteriorhodopsin, the light-driven proton pump from *Halobacterium halobium*. Upon illumination the bacteriorhodopsin pumps protons into the vesicles, resulting in the formation of a membrane potential. This membrane potential can drive ATP synthesis catalyzed by the calcium ATPase. By mechanically chopping the actinic light, a periodic perturbation is created about a steady-state membrane potential. This steady-state potential is independent of chopping frequency over the ranges used and provides a constant chemiosmotic potential. The small, periodic component of the membrane potential perturbs the coupled ATP hydrolysis equilibrium of the ATPase. Although the calcium concentration is identical on both sides of the membrane, the internal calcium will have a higher chemical potential as a result of the membrane potential. The response of the system is monitored spectroscopically by using a fluorescent calcium indicator. The modulated amplitude is measured as a function of frequency and analyzed to determine the relaxation times. The detailed amplitude analysis for such a coupled process has been discussed previously (Dewey, 1987). Since the bacteriorhodopsin response time can be determined experimentally, it is possible under a wide range of conditions to deconvolute the response of the ATPase from that of the proton pump. The relaxation times of calcium transport catalyzed by the calcium ATPase were determined as a function of phosphate and ADP concentration. This allowed accurate rate constants to be determined for the chemiosmotic-coupled ATP synthesis process.

[1] Abbreviations: ATPase, adenosinetriphosphatase; ADP, adenosine 5′-diphosphate; ATP, adenosine 5′-triphosphate; MOPS, 3-(*N*-morpholino)propanesulfonic acid; indo-1, 2-[4-[bis(carboxymethyl)-amino]-3-[2-[2-[bis(carboxymethyl)amino]-5-methylphenoxy]ethoxy]-phenyl]indole-6-carboxylic acid; Tricine, *N*-[tris(hydroxymethyl)-methyl]glycine; ANS, 8-anilino-1-naphthalenesulfonic acid magnesium salt.

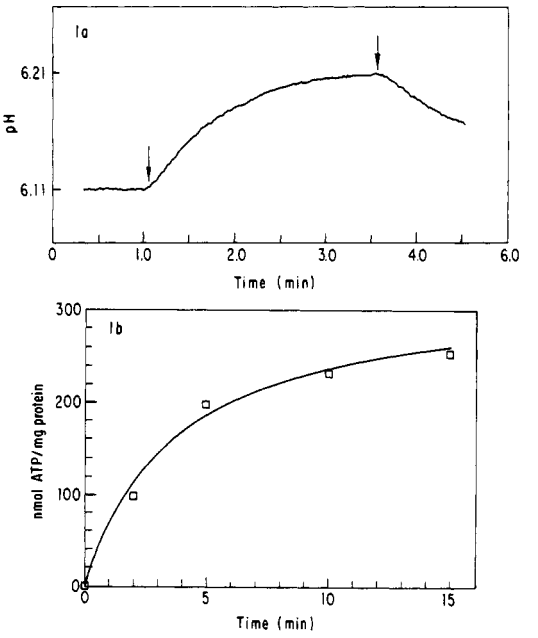

FIGURE 1: Activity assays for double reconstituted vesicles. (a) A plot of pH change due to light-driven proton transport activity of bacteriorhodopsin versus time. The first arrow indicates the start of actinic illumination and the second arrow indicates the end of illumination. The 1-mL reaction mixture contained double reconstituted vesicles (5 mg of asolectin, 0.11 mg of bacteriorhodopsin, 0.21 mg of calcium ATPase) in distilled water. The temperature was 21 °C. (b) Net ATP synthesis by the calcium ATPase driven by bacteriorhodopsin versus time of actinic illumination. Specific activity is calculated per milligram of ATPase. The reaction mixture is identical with (a) with the addition of the 750 μM MgADP complex, 60 mM KCl, 10 mM NaCl, 2.5 mM $MgCl_2$, 10 mM MOPS, 1.4 μM $CaCl_2$, and 2.5 mM KH_2PO_4.

Materials and Methods

Chemicals and Protein Purification. Octyl glucoside (*n*-octyl β-D-glucopyranoside), ADP, luciferase ATP assay mix, and valinomycin were obtained from Sigma Chemical Co. 9-Aminoacridine and ANS were from Eastman, and asolectin (soybean phospholipid) was from Associated Concentrates. Indo-1 was purchased from Molecular Probes. All other reagents were of reagent grade, and all solutions were made in deionized water. The sarcoplasmic reticulum calcium ATPase was purified from rabbit skeletal muscle by using a modification (Banerjee et al., 1979) of the procedure of MacLennan (1970). *H. halobium* S-9 was grown on defined medium (Lanyi & MacDonald, 1979), and purple membrane was purified by using a sucrose step gradient (Becher & Cassim, 1975).

Double Reconstituted Vesicles. The calcium ATPase and bacteriorhodopsin were simultaneously reconstituted into phospholipid vesicles by using the octyl glucoside dilution technique. Vesicles were formed by sonicating 20 mg/mL asolectin to clarity in a bath sonicator. All buffers contained 0.10 M KCl and 50 mM Tricine, pH 7.75. Bacteriorhodopsin and the calcium ATPase were added to this solution to give a final concentration of 0.37 and 0.56 mg/mL, respectively. Octyl glucoside was added to give a final concentration of 48.3 mM, and the mixture was incubated in the dark on ice for 15 min. The octyl glucoside was removed by diluting the vesicles 15-fold and spinning the vesicles at 180000*g* for 60 min. The pellet was then taken up in 25 mL of deionized water and centrifuged as before. This final pellet was taken up in the buffer of choice and dialyzed overnight. These vesicles showed light-driven proton transport activity as demonstrated in Figure 1. This activity was assayed by using a pH electrode as

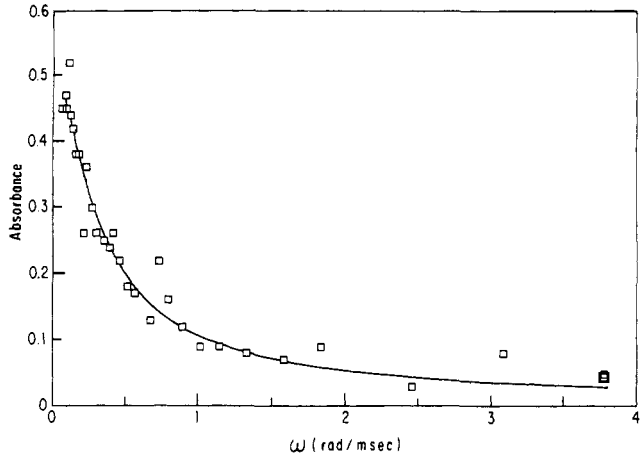

FIGURE 2: Plot of pH indicator absorbance amplitudes versus chopper frequency of actinic light. The 2.0-mL sample contained 0.3 mL of double reconstituted vesicles (0.13 mg/mL ATPase, 0.07 mg/mL bacteriorhodopsin, 3 mg/mL asolectin), and concentrations for other species were 102 mM KCl, 4.25 mM $MgCl_2$, 17.0 mM NaCl, 4.25 mM KH_2PO_4, 375 μM MgADP, and 1.4 μM $CaCl_2$. Data points were obtained by monitoring the absorbance signal of 50 μM *p*-nitrophenol. The theoretical line was obtained by nonlinear least-squares fit to eq 1.

described previously (Racker & Stoeckenius, 1974). The actinic light consisted of an ELH 300-W lamp filtered with Corning CS 3-60 and 1-75 filters. Light-driven ATP synthesis activity was also demonstrated by illuminating the vesicles in the presence of 750 μM MgADP, 2.5 mM $MgCl_2$, 2.5 mM KH_2PO_4, 60 mM KCl, 10 mM NaCl, and 10 mM MOPS. After fixed periods of illumination the reaction was quenched by addition of 180 μL of 1.5 M nitric acid. The mixture was spun at 8130*g*, and the supernatant was assayed for ATP with the luciferase assay at pH 7.8 with identical conditions as described previously (Lundin & Thore, 1975). Luminescence was monitored at 550 nm with a Spex Fluorolog II spectrometer. Figure 1 indicates that ATP production reaches a steady-state level after 10 min of illumination. The ATP synthesis activity shown by this preparation in the linear region of Figure 1 is low compared with photosynthetic systems such as the chloroplast thylakoids (Portis & McCarty, 1974). However, it is comparable to those obtained with a similar system of the chloroplast ATPase reconstituted with bacteriorhodopsin (Dewey & Hammes, 1981b). Coreconstitution of both proteins appears to give the best synthesis activity. To date, separate sequential reconstitution procedures have not yielded preparations of high activity.

Phase-Lifetime and Fluorescence Spectroscopy. Amplitude dispersion curves for various kinetic processes were measured with the phase-lifetime spectrometer described previously (Hasselbacher et al., 1986). The light-driven proton transport kinetics of bacteriorhodopsin in the reconstituted system was determined in unbuffered solutions by monitoring the absorbance signal at 400 nm of *p*-nitrophenol. This signal was corrected for interference from the bacteriorhodopsin photocycle as described previously (Sinton & Dewey, 1987). The absorbance as a function of frequency is shown in Figure 2. The relaxation time for proton transport, τ_D, was determined by fitting the observed frequency dependence to the equation (Dewey, 1987)

$$A = \sum_{n=0} \frac{[A] \sin [(2n + 1)(\pi/2 + \phi_0) - \phi_n]}{(2n + 1)^2[1 + \omega^2\tau_D^2(2n + 1)^2]^{1/2}} \quad (1)$$

where the summation over n represents the harmonics of the response function and can be adequately represented by truncating the series at $n = 50$. The quantities [A] and τ_D represent the amplitude and lifetime of the relaxation process, respectively, and are obtained from a nonlinear least-squares fit of the data to eq 1. The phase shift for each harmonic is given by $\tan \phi_n = (n + 1)\omega\tau_D$. Equation 1 accounts for the harmonic sensitivity of the specific "lock-in" amplifier used in this study. Typically, the relaxation time of the proton transport process of bacteriorhodopsin ranges from 2 to 6 ms. These times are determined for each vesicle preparation.

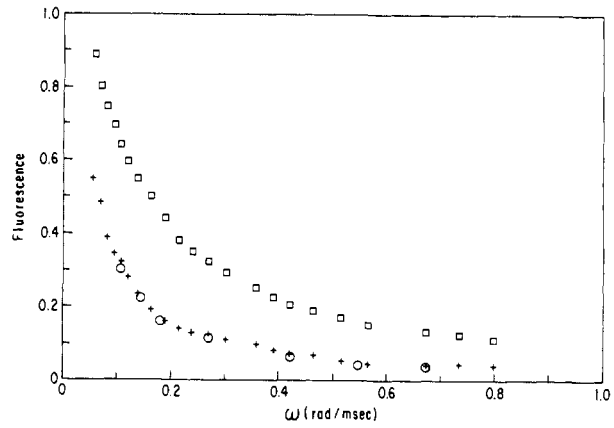

FIGURE 3: Plot of indo-1 (calcium indicator) fluorescence amplitudes versus chopper frequency of actinic light. The 2.0-mL sample contained 102 mM KCl, 4.25 mM $MgCl_2$, 17.0 mM NaCl, 4.25 mM KH_2PO_4, 375 μM MgADP, 1.4 μM $CaCl_2$, and 17 mM MOPS. (□) The sample contained 0.3 mL of double reconstituted vesicles. (+) The sample contained 0.3 mL of double reconstituted vesicles and 30 μM valinomycin. (○) The sample contained 0.3 mL of reconstituted vesicles with bacteriorhodopsin but not with calcium ATPase.

The calcium amplitude dispersion curves were measured in a reaction buffer consisting of 102 mM KCl, 17 mM NaCl, 4.25 mM $MgCl_2$, 17 mM MOPS, and 1.4 μM Ca^{2+}. The concentrations of MgADP and phosphate were systematically varied. The fluorescent calcium indicator indo-1 was excited at 340 nm, and the fluorescence signal was filtered with a Oriel 400-nm narrow band-pass filter. Figure 3 shows a typical amplitude dispersion curve for this fluorescence. As a control, the fluorescence signal was measured after valinomycin was added to dissipate the membrane potential. The amplitude of the resulting signal was reduced but not eliminated (see Figure 3). This signal was identical with the one obtained with vesicles containing bacteriorhodopsin and no calcium ATPase (Figure 3). This residual signal is most likely due to inner filter effects of the bacteriorhodopsin photocycle on the indo-1 fluorescence. The fact that the signal in the presence of valinomycin is identical with the "background" signal is very important as it indicates that the pH gradient is not affecting calcium transport. Subsequently, all measurements subtracted the signal with valinomycin from the signal without it. The resulting amplitude dispersion curve was fit to (Dewey, 1987)

$$F(\omega) = \sum_{n=0} \frac{[F] \sin [(2n + 1)(\pi/2 + \phi_0 + \phi_{D,0}) - \phi_n - \phi_{D,n}]}{(2n + 1)^2[1 + \omega^2\tau^2(2n + 1)^2]^{1/2}[1 + \omega^2\tau_D^2(2n + 1)^2]^{1/2}} \quad (2)$$

where $\tan \phi_n = (2n + 1)\omega\tau$ and $\tan \phi_{D,n} = (2n + 1)\omega\tau_D$ define the phase angles for the chemiosmotic process and the proton pump, respectively. The amplitude [F] and the relaxation time τ are determined from a nonlinear least-squares fit. The value of τ_D was determined from the proton transport experiment. Again, the series could be truncated at $n = 50$ without loss of accuracy.

To determine if the steady-state level of the chemiosmotic potential was changing with the chopping frequency of actinic

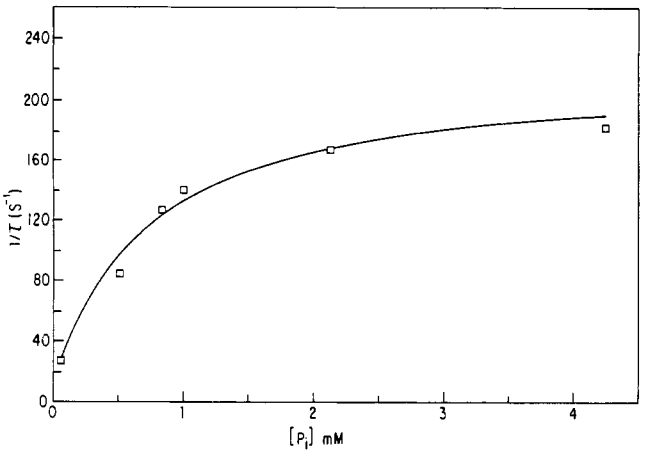

FIGURE 4: Plot of the reciprocal relaxation time of calcium transport versus phosphate concentration. The experiment conditions were identical with those in Figure 3 except the reaction mixture contained 17 mM MOPS. The solid line was obtained by fitting the data to the function form of eq 4. Each data point represents the average of at least three experiments.

light, several steady-state fluorescence experiments were performed. These used the identical actinic excitation source and chopper as in the kinetic measurements. However, the steady-state fluorescence was measured with a Perkin-Elmer MPF-3L that had been adapted to allow actinic illumination. The steady-state levels of 9-aminoacridine and ANS were measured as a function of frequency. 9-Aminoacridine is a monitor of the pH gradient (Schuldiner et al., 1972) and was excited at 403 nm while the emission at 465 nm was observed. The ANS signal is a measure of membrane potential (Waggoner, 1979). It was excited at 380 nm and emission was observed at 480 nm. In both cases the fluorescence was independent of chopping frequency, indicating that the steady-state pH gradient and membrane potential were not changing. This was also true for vesicles in the presence of ADP and phosphate. This latter control was very important as it shows that frequency-dependent variations in the calcium ATPase's activity were not large enough to significantly alter the steady-state membrane potential. Although these experiments provide information concerning the steady-state levels of the pH gradient and membrane potential, it is extremely difficult to quantitate the absolute values of these quantities. Future work will concentrate on the measurement of these parameters.

Results

All of the amplitude dispersion curves for calcium transport could be fit to a single relaxation process. Figure 4 shows a plot of the reciprocal relaxation time of calcium transport versus phosphate concentration at 375 μM ADP. This plot shows a linear region at low phosphate and saturation at high phosphate. This is characteristic of a process in which a fast step is followed by a slow one. Thus, the simplest possible interpretation would use the mechanism

$$E + P_i \underset{k_{-1}}{\overset{k_1}{\rightleftharpoons}} EP_i \underset{k_{-2}}{\overset{k_2}{\rightleftharpoons}} X \qquad (3)$$

where E represents the enzyme with bound ADP. Subsequent steps are uncoupled from the relaxation as a result either of being too slow or of not contributing to the amplitude of the calcium signal. The relaxation time for the mechanism in eq 3 is

$$1/\tau = k_{-2} + k_2k_1([E] + [P_i])/[k_1([E] + [P_i]) + k_{-1}] \qquad (4)$$

The value of [E] is much less than the phosphate concentration and is ignored throughout. The intercept gives a k_{-2} value of

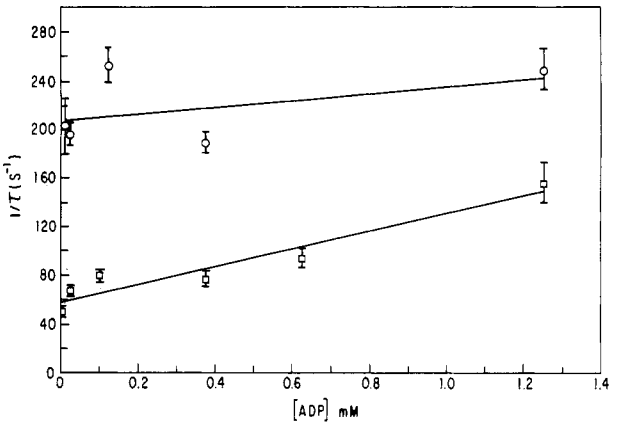

FIGURE 5: Plot of the reciprocal relaxation time of calcium transport versus ADP concentration. The concentration of phosphate, 4.25 mM for the upper line, was 4.25 and 0.5 mM for the lower line. Solid lines are linear least-squares fits. All other experimental conditions were the same as in Figure 4. Error bars are determined from the nonlinear least-squares fitting routine.

22 s^{-1}. The saturation level equals ($k_2 + k_{-2}$) and is 190 s^{-1}. This gives a value of 168 s^{-1} for k_2 and an equilibrium constant of 8.6 for the isomerization step. The slope in the linear region is 1.2 10^5 M^{-1} s^{-1} and is equal to k_2K_1, where K_1 is the equilibrium constant for phosphate association. From these values a phosphate dissociation constant ($1/K_1$) of 1.4 mM is calculated. This compares favorably with the Michaelis constant for phosphate determined under a variety of transmembrane calcium gradients (Fagan & Dewey, 1985). These values ranged from 1 to 4 mM.

Figure 5 shows the dependence of the reciprocal relaxation time on ADP concentration. At saturating phosphate (4.25 mM) the reciprocal relaxation times are weakly dependent on [ADP] and the slope of the curve could not be accurately determined. At lower phosphate (0.5 mM) the reciprocal relaxation time is linearly dependent on ADP with an intercept of 60 s^{-1} and a slope of 0.7 10^5 M^{-1} s^{-1}. The dependence of the ADP slopes and intercepts on phosphate cannot be interpreted by a simple ordered mechanism. A random sequential mechanism, as observed in the steady-state kinetics (Fagan & Dewey, 1985), gives complicated phosphate dependences for these parameters. This mechanism can be reconciled with the transient data with some simplifying assumptions. It is given by

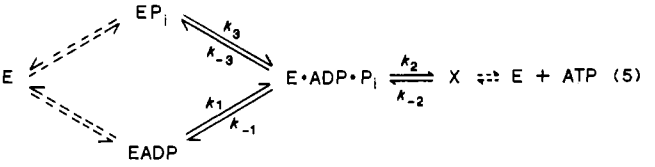

where the dotted lines represent steps that are uncoupled from the observed relaxation process and the isomerization step is slow relative to the two bimolecular steps. This scheme gives the expression:

$$1/\tau = \frac{k_1k_2([EADP] + [P_i])}{k_{-1} + k_1([EADP] + [P_i])} + \frac{k_{-2}k_3([EP_i] + [ADP])}{k_{-3} + k_3([EP_i] + [ADP])} + \frac{k_1k_{-3}(k_{-2} - k_2)([EADP] + [P_i])}{\{k_{-1} + k_1([EADP] + [P_i])\}\{k_{-3} + k_3([EP_i] + [ADP])\}} \qquad (6)$$

Due to their low levels, terms involving enzyme species are dropped. Also, because the level of ATP synthesis is low, it is assumed that the steady-state concentrations of ADP and P_i are not significantly different from the initial concentrations. The value of K_1 may be calculated as in eq 4 and gives an

identical result. The values of k_2 and k_{-2} are no longer uniquely determined from the phosphate dependence alone. Equation 6 predicts the linear ADP dependence when $k_{-3} > k_3[ADP]$. It gives an intercept of $k_{-2}K_1[P_i]/(1 + K_1[P_i])$ and a slope of $k_{-2}K_3$. Using the K_1 of 722 M^{-1} and the experimental ADP slope and intercept at 0.5 mM phosphate of 0.7 10^5 M^{-1} s^{-1} and 60 s^{-1}, respectively, gives a k_{-2} of 227 s^{-1} and a K_3 of 309 M^{-1} (K_d of 3.2 mM). This dissociation constant is higher than the observed Michaelis constant (30–60 μM) (Fagan & Dewey, 1985) but is closer to the ADP binding constant to a phosphoenzyme form of 0.73 mM (Pickart & Jencks, 1984). Since these comparisons are made to slightly different parameters under different buffer conditions, these results are not inconsistent. With the previously determined values and the value for the intercept on the phosphate plot, a value of 67 s^{-1} is calculated for k_2. This gives an equilibrium constant of 0.3 for the isomerization reaction.

Discussion

Phase-lifetime spectroscopy has been used to measure chemical relaxation in a chemiosmotic-coupled system. Phospholipid vesicles were prepared in which both bacteriorhodopsin and the calcium ATPase are functionally reconstituted into the membrane. Upon illumination the bacteriorhodopsin transports protons and forms both a pH and membrane potential. This membrane potential can then be used to perturb the equilibrium of ATP hydrolysis/synthesis coupled to calcium transport. The finite response time of bacteriorhodopsin limits the time resolution of this modulation technique. By separately measuring the kinetics of light-driven proton pumping, it is possible to deconvolute the response of the ATPase from that of the proton pump. Simulated amplitude dispersion curves show that even when the coupled process is slightly faster than the driving process, it is still possible to resolve its kinetics (Dewey, 1987). Consequently, this technique allows the relaxation processes to be resolved on the millisecond time scale. This resolution should be adequate for measuring most ion transport processes.

The initial results obtained by this technique for the calcium ATPase are encouraging. Relaxations involving ADP and phosphate addition to the enzyme have been resolved. The binding constants for these two species could be calculated from the kinetic data and compare favorably with previous results. This provides added confidence in the validity of this approach. The dependence of the reciprocal relaxation time on both phosphate and ADP was interpreted with a random sequential mechanism. A more extensive investigation of these dependences is under way to firmly establish this mechanism. However, the key feature that this technique can provide is the dependence of calcium transport on the membrane potential. This information will be invaluable in elucidating the step that is directly involved in calcium translocation. The identification of the calcium transport step in the reaction mechanism has been the topic of considerable recent controversy (Froehlich & Heller, 1985; Petithory & Jencks, 1986). Previous mechanisms may not be correct because detergent-solubilized enzyme was used and this may effect the kinetics (Kosk-Kosicka et al., 1983). This technique provides a means to address such problems.

References

Auslaender, W., & Junge, W. (1975) *FEBS Lett. 59*, 310–315.

Banerjee, R., Epstein, M., Kandrack, M., Zimniak, R., & Racker, E. (1979) *Membr. Biochem. 2*, 283–296.

Becher, B. M., & Cassim, J. Y. (1975) *Prep. Biochem. 5*, 161–178.

Dewey, T. G. (1987) *Biophys. J. 51*, 809–815.

Dewey, T. G., & Hammes, G. G. (1981a) *Proc. Natl. Acad. Sci. U.S.A. 78*, 7422–7425.

Dewey, T. G., & Hammes, G. G. (1981b) *J. Biol. Chem. 256*, 8941–8946.

Fagan, M. H., & Dewey, T. G. (1985) *J. Biol. Chem. 260*, 6147–6152.

Froehlich, J. F., & Heller, P. F. (1985) *Biochemistry 24*, 126–136.

Hasselbach, W. (1978) *Biochim. Biophys. Acta 515*, 23–53.

Hasselbacher, C. A., Preuss, D. K., & Dewey, T. G. (1986) *Biochemistry 25*, 668–676.

Knox, B. E., & Tsong, T. Y. (1984) *J. Biol. Chem. 259*, 4757–4763.

Kosk-Kosicka, D., Kurzmack, M., & Inesi, G. (1983) *Biochemistry 22*, 2559–2567.

Lanyi, J. K., & MacDonald, R. E. (1979) *Methods Enzymol. 56*, 398–407.

Lundin, A., & Thore, A. (1975) *Anal. Biochem. 66*, 47–63.

MacLennan, D. H. (1970) *J. Biol. Chem. 245*, 4508–4518.

Petithory, J. R., & Jencks, W. P. (1986) *Biochemistry 25*, 4493–4497.

Pickart, C. M., & Jencks, W. P. (1984) *J. Biol. Chem. 259*, 1629–1643.

Portis, A. R., Jr., & McCarty, R. E. (1974) *J. Biol. Chem. 249*, 6250–6254.

Racker, E., & Stoeckenius, W. (1974) *J. Biol. Chem. 249*, 662–663.

Schuldiner, S., Rottenberg, H., & Avron, M. (1972) *Eur. J. Biochem. 25*, 64–70.

Sinton, M. H., & Dewey, T. G. (1987) *Biophys. J.* (submitted for publication).

Tsong, T. Y., & Astumian, R. D. (1986) *Bioelectrochem. Bioenerg. 15*, 457–476.

Waggoner, A. S. (1979) *Annu. Rev. Biophys. Bioeng. 8*, 47–68.